
Selectivity considered harmful: evaluating the causal impact of class selectivity in DNNs

Matthew L. Leavitt^{1,2} Ari S. Morcos¹

Abstract

Class selectivity—typically defined as how different a neuron’s responses are across different classes of stimuli or data samples—is a common metric used to interpret the function of individual neurons in biological and artificial neural networks. However, it remains an open question whether it is necessary and/or sufficient for deep neural networks (DNNs) to learn class selectivity in individual units. In order to investigate the causal impact of class selectivity on network function, we directly regularize for or against class selectivity. Using this regularizer, we were able to reduce mean class selectivity across units in convolutional neural networks by a factor of 2.5 with no impact on test accuracy, and reduce it nearly to zero with only a small ($\sim 2\%$) change in test accuracy. In contrast, increasing class selectivity beyond the levels naturally learned during training had rapid and disastrous effects on test accuracy. These results indicate that class selectivity in individual units is neither sufficient nor strictly necessary for DNN performance, and more generally encourage caution when focusing on the properties of single units as representative of the mechanisms by which DNNs function.

1. Introduction

Our ability to understand deep learning systems lags considerably behind our ability to obtain practical outcomes with them. A breadth of approaches have been developed in attempts to better understand deep learning systems and render them more comprehensible to humans (Yosinski et al., 2015; Bau et al., 2017; Olah et al., 2018; Hooker et al., 2019). Many of these approaches are inspired by techniques for understanding a different complex system that has also

proven extremely successful at solving a variety of challenging problems: the nervous system. Examining the properties of single neurons in order to gain understanding about the networks in which they’re embedded is a common practice in neuroscience (Sherrington, 1906; Adrian, 1926; Granit, 1955; Barlow, 1972; Kandel et al., 2000), and has also been widely applied in deep learning (Erhan et al., 2009; Zeiler & Fergus, 2014; Karpathy et al., 2016; Amjad et al., 2018; Lillian et al., 2018; Dhamdhere et al., 2019).

The selectivity of individual units’ activations across inputs (often referred to as "tuning" in neuroscience) has been of particular interest to researchers of both artificial (Zhou et al., 2015; Olah et al., 2017; Meyes et al., 2019; Na et al., 2019; Zhou et al., 2019) and biological (Hubel & Wiesel, 1962; De Valois et al., 1982; Britten et al., 1992; Moody et al., 1998; Kandel et al., 2000) neural networks. This focus on individual neurons makes intuitive sense as the tractable, semantic nature of selectivity is extremely alluring; some measure of selectivity in individual units is often provided as an explanation of "what" a network is "doing."

The report of neurons in the human medial temporal lobe selective for images and phrases relating to famous people and places (Quiñ Quiroga et al., 2005), and of a neuron selective for sentiment in an LSTM network trained on a word prediction task (Radford et al., 2017) both influenced many subsequent studies, demonstrating the widespread, intuitive appeal of "selectivity." Finding intuitive ways of representing the workings of DNNs (and complex systems more generally) is essential for making them understandable and accountable, but we must ensure that our approaches are based on meaningful properties of the system. Recent studies have begun to address this issue by investigating the relationships between selectivity and critical measures of network function such as generalization and robustness to perturbation (Morcos et al., 2018b; Zhou et al., 2018; Dalvi et al., 2019), and selectivity has been used as the basis for targeted modulation of neural network functionality through individual units (Bau et al., 2019a;b).

However there is also growing evidence from experiments in both neuroscience (Leavitt et al., 2017; Zylberberg, 2018; Insanally et al., 2019) and deep learning (Fong & Vedaldi,

¹Facebook AI Research, Menlo Park, California ²Work performed as part of the Facebook AI Residency program. Correspondence to: Matthew L. Leavitt <ito@fb.com>, Ari S. Morcos <arimorcos@fb.com>.

2018; Morcos et al., 2018b; Gale et al., 2019; Donnelly & Roegiest, 2019) that selectivity may not be as important as once thought. Previous studies examining the functional role of selectivity in DNNs have often measured how selectivity mediates the effects of ablating single units, or used indirect, correlational approaches that modulate selectivity indirectly (e.g. batch norm) (Morcos et al., 2018b; Zhou et al., 2018; Lillian et al., 2018; Meyes et al., 2019). Single unit ablation in trained networks can be a useful approach for examining whether reducing selectivity negatively affects network performance, but it has two limitations: it cannot address whether the *presence* of selectivity is beneficial, nor whether networks *need to learn* selectivity to function properly.

We were motivated by these issues to pursue a series of experiments investigating the relevance of class selectivity in artificial neural networks. To do so, we introduced a term to the loss function that allows us to directly regularize for or against class selectivity, effectively giving us a single knob to control class selectivity in the network. This approach serves as the basis for a series of experiments allowing us to evaluate the causal impact of class selectivity on DNN performance. Our findings are as follows:

- Class selectivity is not strictly necessary for networks to function. We reduced the mean class selectivity of units in a network by a factor of ~ 2.5 with no impact on test accuracy, and by a factor of ~ 20 —nearly to a mean of 0—with only a 2% change in test accuracy.
- Our regularizer does not simply cause networks to preserve class-selectivity by rotating it off of unit-aligned axes (i.e. by distributing selectivity linearly across units), but rather seems to suppress selectivity more generally. This demonstrates the viability of low-selectivity representations *across* units.
- We show that regularizing to increase class selectivity has rapid and catastrophic effects on performance. Trained networks seem to be perched precariously at a performance cliff with regard to class selectivity. These results indicate that the levels of class selectivity learned by individual units are at the limit of what doesn't impair the network.

Our findings collectively demonstrate that class selectivity in individual units is neither necessary nor sufficient for DNNs to function, and in some cases, can actually be harmful. More broadly, our results encourage caution when focusing on the properties of single units as representative of the mechanisms by which DNNs function.

2. Related work

2.1. Selectivity in deep learning

Examining some form of selectivity in individual deep neural network (DNN) units forms the bedrock of many approaches to interpretability. Sometimes the goal is to visualize selectivity, which has been pursued using a breadth of approaches. These include identifying the input sample(s) (e.g. images) or sample subregions that maximally activate a given neuron (Zhou et al., 2015), and a number of optimization-based methods for generating samples that maximize a unit's activation (Erhan et al., 2009; Zeiler & Fergus, 2014; Simonyan et al., 2014; Yosinski et al., 2015; Nguyen et al., 2016; Olah et al., 2017; 2018). Single units in models trained to solve natural language processing tasks have been found to exhibit selectivity for syntactical and semantic features (Karpathy et al., 2016; Na et al., 2019). The "sentiment-selective neuron" reported in Radford et al. (2017) is a particularly recognized example.

The relationship between individual unit selectivity and various measures of DNN performance have been examined in prior studies (e.g. Amjad et al. (2018); Meyes et al. (2019)), but the conclusions are not always concordant. Morcos et al. (2018b) found that networks that generalize to the test set well tend to have units with lower class selectivity compared to networks that generalize poorly. They also found that the performance loss from ablating an individual unit tends not to be correlated—and in some instances is even anti-correlated—with that unit's class selectivity.

In a follow-up study, Zhou et al. (2018) found that ablating class-selective units impairs classification accuracy for specific classes (though interestingly, not always the same class the unit was selective for in the first place), but a compensatory increase in accuracy for other classes can often leave overall accuracy unaffected. Ukita (2018) found that orientation selectivity in individual units is correlated with generalization performance in convolutional neural networks (CNNs), and that ablating highly orientation-selective units impairs classification accuracy more than ablating units with low orientation-selectivity. It is worth noting, however, that while orientation selectivity and class selectivity can both be considered types of feature selectivity, orientation selectivity is far less abstract and focuses on specific properties of the image (e.g., oriented edges) rather than semantically meaningful concepts and classes. Nevertheless, this study still demonstrates the importance of some types of selectivity.

Variable results have also been observed in models trained on NLP tasks. Dalvi et al. (2019) found that ablating units selective for linguistic features causes greater performance deficits on than ablating less-selective units, while Donnelly & Roegiest (2019) found that ablating the "sentiment neuron" of Radford et al. (2017) has equivocal effects on

performance. These findings seem challenging to reconcile. Furthermore, single unit ablation studies can only address whether class selectivity affects performance in trained networks, and not whether network performance requires individual units to *learn* class selectivity.

2.2. Selectivity in neuroscience

Measuring the responses of single neurons to a relevant set of stimuli began in the early 20th century (Sherrington, 1906; Adrian, 1926) and developed into one of the most widely used and productive approaches to understanding the nervous system (Granit, 1955; Hubel & Wiesel, 1959; Barlow, 1972; Kandel et al., 2000). Hubel and Wiesel’s research, for which they shared the 1981 Nobel Prize, systematically characterized neuronal tuning in primary visual cortex and how experience shapes the development of the visual system (Hubel & Wiesel, 1959; 1962; Hubel, 1982; Wiesel, 1982). Single neuron measures of selectivity are the canonical first-order description of a neural system. However, recent experimental findings and computational models have raised doubts about the necessity of selectivity for high-fidelity representations in neuronal populations.

Leavitt et al. (2017) found that non-selective neurons in primate prefrontal cortex can increase the information content of a neuronal population. They do so by modifying the neuronal population’s covariance structure in a manner that increases discriminability between representations. Insanally et al. (2019) reported similar findings in rat auditory cortex, and Zylberberg (2018) in mouse visual cortex. The latter study also derived a mathematical model demonstrating that populations composed of a mixture of selective and non-selective neurons can encode stimulus information better than populations composed exclusively of selective neurons. Indeed, neuroscience as a field seems to be moving beyond characterizing neural systems at the level of single neurons, towards population-level phenomena (Shenoy et al., 2013; Raposo et al., 2014; Fusi et al., 2016; Morcos & Harvey, 2016; Pruszyński & Zylberberg, 2019; Heeger & Mackey, 2019; Saxena & Cunningham, 2019).

Single unit selectivity-based approaches are ubiquitous in researchers’ attempts to understand artificial and biological neural systems, but growing evidence has led to questions about the importance of focusing on selectivity and its role in DNN function. These factors, combined with the limitations of previous approaches, lead to the question: is class selectivity necessary and/or sufficient for DNN function?

3. Approach

Networks naturally seem to learn solutions that result in class-selective individual units. We examined whether learning class-selective representations in individual units is actu-

ally necessary for networks to function properly. Motivated by the limitations of single unit ablation techniques and the indirectness of using batch norm or dropout to modulate class selectivity (e.g. Morcos et al. (2018b); Zhou et al. (2018); Lillian et al. (2018); Meyes et al. (2019)), we developed an alternative approach to examining the necessity of class selectivity for network performance. By adding a term to the loss function that serves as a regularizer to suppress (or increase) class selectivity, we demonstrate that it is possible to directly modulate the amount of class selectivity in all units in aggregate. We then used this approach as the basis for a series of experiments in which we modulated levels of class-selectivity across individual units and measured the resulting effects on the network.

Unless otherwise noted: all experimental results were derived from the test set with the parameters from the epoch that achieved the highest validation set accuracy over 200 training epochs; 20 replicates with different random seeds were run for each hyperparameter set; error bars and shaded regions denote bootstrapped 95% confidence intervals.

3.1. Models and dataset

Our experiments were performed on ResNet20 (He et al. (2016); code modified from Idelbayev (2020)) and a VGG16-like network (Simonyan & Zisserman, 2015), both trained on CIFAR10 (Krizhevsky, 2009). Additional details about hyperparameters, data, training, and software are in Appendix A.1. Code and packages for conducting specific analyses are referenced in the relevant **Approach** subsection.

3.2. Defining class selectivity

There are a breadth of approaches for quantifying class selectivity in individual units (Moody et al., 1998; Zhou et al., 2015; Li et al., 2015; Zhou et al., 2018; Gale et al., 2019). We chose the neuroscience-inspired approach of Morcos et al. (2018b) because it is similar to many widely-used metrics, easy to compute, and most importantly, differentiable (the utility of this will be addressed in the next section). We also confirmed the efficacy of our regularizer using a different selectivity metric (see Appendix A.5). For a single convolutional feature map (which we refer to as a "unit"), the activation in response to a single sample was averaged across all elements of the filter map. Then the class-conditional mean activation (i.e. the mean activation for each class) was calculated across all samples in the test set, and the class selectivity index was calculated as follows:

$$selectivity = \frac{\mu_{max} - \mu_{-max}}{\mu_{max} + \mu_{-max}} \quad (1)$$

where μ_{max} is the largest class-conditional mean activation and μ_{-max} is the mean response to the remaining (i.e. non-

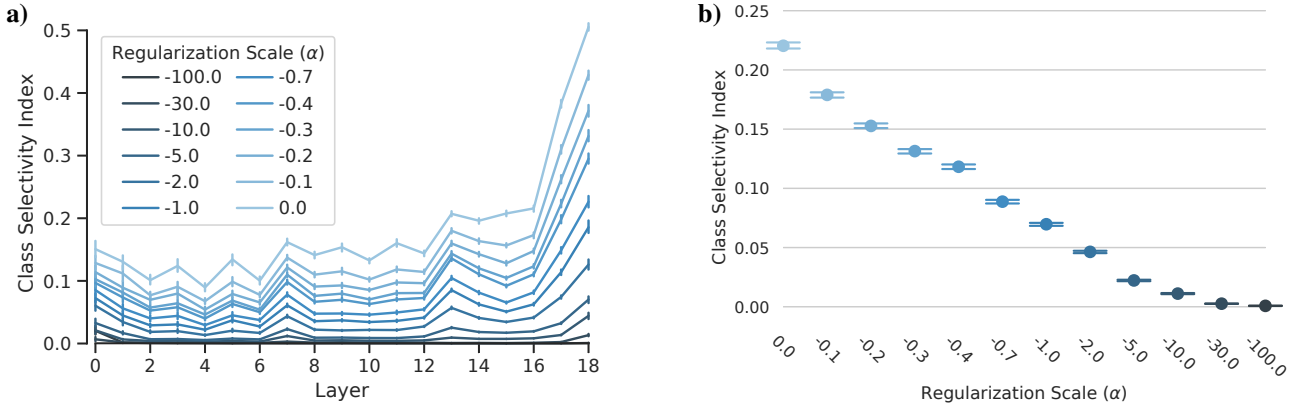


Figure 1: Manipulating class selectivity by regularizing against it in the loss function. (a) Mean class selectivity index (y-axis) as a function of layer (x-axis) for different regularization scales (α ; denoted by intensity of blue) for ResNet20. (b) Similar to (a), but mean is computed across all units in a network instead of per layer. Error bars denote bootstrapped 95% confidence intervals.

μ_{max}) classes. The selectivity index can range from 0 to 1. A unit with identical average activity for all classes would have a selectivity of 0, and a unit that only responded to a single class would have a selectivity of 1.

As noted in Morcos et al. (2018b), this selectivity index is not a perfect measure of information content in single units. For example, a unit with a small amount of information about many classes would have a small class selectivity index. However, it achieves the goal of identifying units that are class-selective in similarly intuitive way to those examined in prior studies (Zhou et al., 2018). And most importantly, it is differentiable.

3.3. A single knob to control class selectivity

Because the class selectivity index is differentiable, we can insert it into the loss function, allowing us to directly regularize against (or for) class selectivity. Our loss function therefore takes the following form:

$$loss = - \sum_c^C y_c \cdot \log(\hat{y}_c) - \alpha \mu_{SI} \quad (2)$$

The left-hand term in the loss function is the traditional cross-entropy between the softmax of the output units and the true class labels, where c is the class index, C is the number of classes, y_c is the true class label, and \hat{y}_c is the predicted class probability. We refer to the right-hand component of the loss function, $-\alpha \mu_{SI}$, as the class selectivity regularizer (or regularizer, for brevity). The regularizer consists of two components: the selectivity term, μ_{SI} , which is defined as

$$\mu_{SI} = \frac{1}{L} \sum_l^L \frac{1}{U} \sum_u^U SI_u \quad (3)$$

where l is a convolutional layer, L is number of layers, u is

a unit (i.e. feature map), U is the number of units in a given layer, and SI_u is the class selectivity index of unit u . Thus the selectivity component of the regularizer is obtained by computing the selectivity index for each unit in a layer, then computing the mean selectivity index across units within each layer, then computing the mean selectivity index across layers. Computing the mean within layers before computing the mean across layers (as compared to computing the mean across all units in the network) mitigates the biases induced by the larger numbers of units in deeper layers. The remaining component in the regularizer is α , the regularizer scale. The sign of α determines whether class selectivity is encouraged or penalized. Negative values of α disincentivize class selectivity in individual units, while positive values promote class selectivity. The magnitude of α controls the contribution of the selectivity term to the overall loss. α thus serves as a single knob with which we can modulate class selectivity across all units in the network in aggregate.

During training, the class selectivity index was computed for each minibatch. For all analyses and results presented here, the class selectivity index was computed across the entire test set, unless otherwise noted.

3.4. Canonical Correlation Analysis

We used Canonical Correlation Analysis (CCA) to examine the effects of class selectivity regularization on representations in neural networks. CCA is a statistical technique that takes two sets of multidimensional variates and finds the linear combinations of these variates that have maximum correlation with each other (Hotelling, 1936). Critically, CCA is invariant to rotation and other invertible affine transformations. CCA has been used in a number of recent studies to analyze and compare representations in (and between) biological and neural networks (Sussillo et al., 2015; Smith et al., 2015; Raghu et al., 2017; Morcos et al., 2018a;

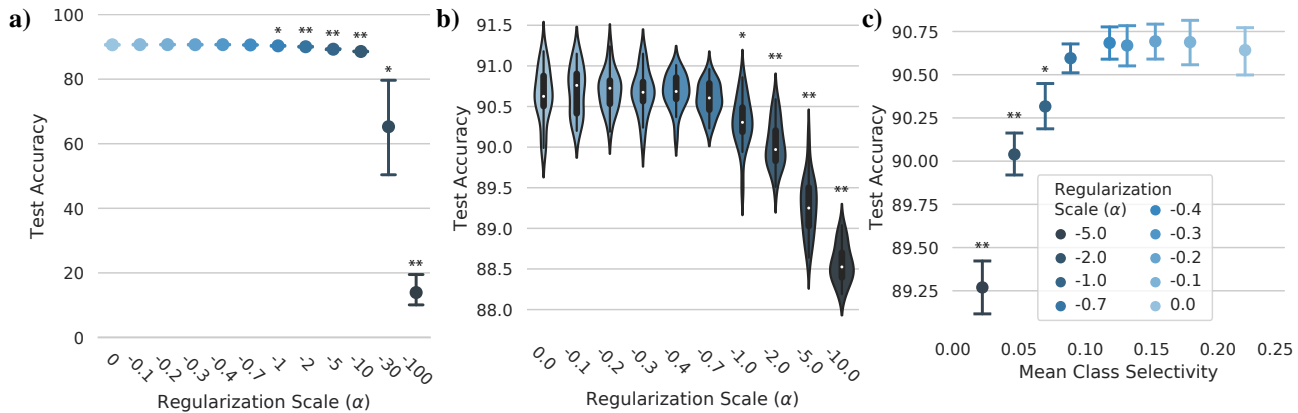


Figure 2: Effects of reducing class selectivity on test accuracy. (a) Test accuracy (y-axis) as a function of regularization scale (α , x-axis and intensity of blue). (b) Identical to (a), but for a subset of α values. The center of each violin plot contains a boxplot, in which the darker central lines denote the central two quartiles. (c) Test accuracy (y-axis) as a function of mean class selectivity (x-axis) for different values of α . Error bars denote 95% confidence intervals. $*p < 0.05$, $**p < 5 \times 10^{-6}$ difference from $\alpha = 0$, t-test, Bonferroni-corrected. All results shown are for ResNet20.

Gallego et al., 2018).

We use projection-weighted CCA (PWCCA), a variant of CCA introduced by Morcos et al. (2018a) that has been shown to be more robust to noise than traditional CCA and other CCA variants. PWCCA generates a scalar value, ρ , that can be thought of as the distance or dissimilarity between two sets of multidimensional variates, L_1 and L_2 . If $L_2 = L_1$, then $\rho_{L_1, L_2} = 0$. Now let R be a rotation matrix. Because CCA is invariant to rotation and other invertible affine transformations, if $L_2 = RL_1$ (i.e. if L_2 is a rotation of L_1), then $\rho_{L_1, L_2} = 0$. In contrast, traditional similarity metrics such as Pearson’s Correlation and cosine similarity would obtain different values if $L_2 = L_1$ compared to $L_2 = RL_1$.¹ For a detailed description of CCA, see Appendix A.2.

4. Results

4.1. Reducing class selectivity without reducing test accuracy

Prior research has yielded equivocal results regarding the importance of class selectivity in individual units. Furthermore, many of these results have been generated either by correlational approaches that modulate selectivity indirectly (e.g. batch norm), or by examining how selectivity mediates the effects of ablating single units. We sidestepped these limitations by regularizing against selectivity directly in the loss function through the addition of the selectivity term (see Approach 3.3 for details), giving us a knob with which to causally manipulate class selectivity. The effect of the

¹We use the PWCCA implementation available [here](#), as provided in Morcos et al. (2018a). We hereafter use CCA to refer to PWCCA unless specifically noted.

regularization term on class selectivity can be seen in Figure 1. Class selectivity across units in a network decreases monotonically as α becomes more negative. We also confirmed our class selectivity regularizer has a similar effect when measured using a different class selectivity metric (see Appendix A.5), indicating that our results are not unique to the metric used in our regularizer. The regularizer thus allows us to examine the causal impact of class selectivity in individual units on test accuracy.

Regularizing against class selectivity could yield one of three possible outcomes: If the previously-reported anti-correlation between selectivity and generalization is also causal, then we should expect test accuracy to increase. However if class selectivity is indeed necessary for high-fidelity class representations, then we should observe a decrease in test accuracy. Finally, if class selectivity is an emergent phenomenon and/or irrelevant to network performance, we should not see any change in test accuracy.

Surprisingly, we observed that selectivity has little—if any—effect on test accuracy, except at extreme regularization scales ($\alpha \leq -30$; Figure 2). As we increase the magnitude of α , mean class selectivity across the network decreases with little impact on test accuracy until mean class selectivity reaches 0.003 at $\alpha = -30$ (Figure 1b; Figure 2a). Reducing class selectivity only begins to have a statistically significant effect on performance at $\alpha = -1.0$ (Figure 2c), at which point mean class selectivity across the network has decreased from 0.22 at $\alpha = 0$ (i.e. no regularization) to 0.07 at $\alpha = -1.0$ —a factor of more than 3 (Figure 2c; $p = 0.03$, Bonferroni-corrected t-test). This implies that the network learns more than three times the amount of class selectivity it needs to achieve maximum test accuracy.

We observed qualitatively similar results for VGG16 (see

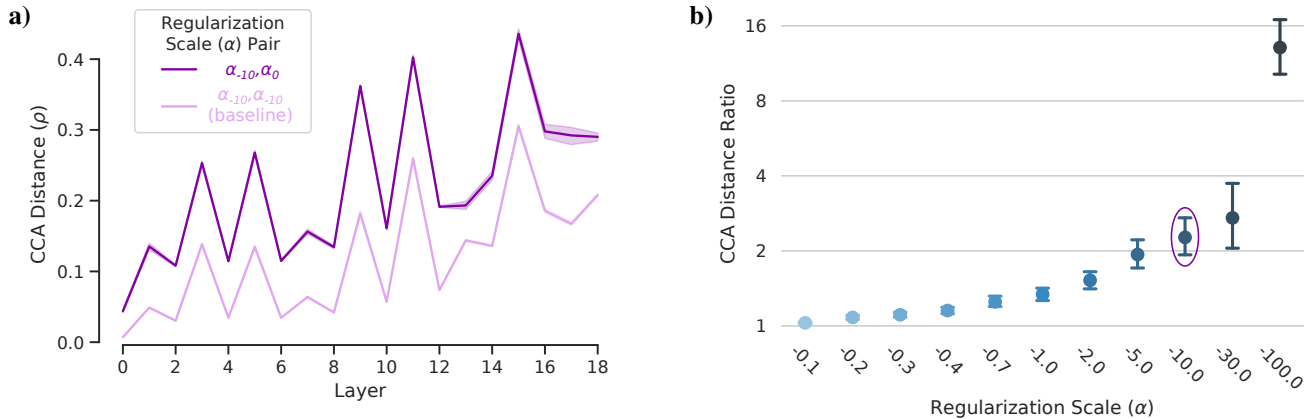


Figure 3: Using CCA to check whether class selectivity is rotated off-axis. (a) Mean CCA distance (ρ , y-axis) as a function of layer (x-axis) between pairs of replicate networks (see Approach 3.4) trained with $\alpha = -10$ (denoted $\rho(\alpha_{-10}, \alpha_{-10})$; light purple), and between pairs of networks trained with $\alpha = -10$ and $\alpha = 0$ (i.e. no class selectivity regularization, denoted $\rho(\alpha_{-10}, \alpha_0)$; dark purple). Shaded region denotes 95% confidence interval. The wide gap between the lines indicates that class selectivity is being suppressed, not simply rotated off-axis. For each layer, we can compute the ratio of $\rho(\alpha_{-10}, \alpha_0) : \rho(\alpha_{-10}, \alpha_{-10})$, which we refer to as the CCA distance ratio. We show this ratio for different values of α in (b), where the CCA distance ratio is averaged across layers (y-axis) and plotted as a function of α (x-axis, intensity of blue). The example from panel a ($\alpha = -10$) is circled in purple. Error bars = 95% confidence intervals. The distance ratio is significantly greater than the baseline for all values of α ($p < 5 \times 10^6$, paired t-test). Results shown are for ResNet20.

Appendix A.4). Although the difference is significant at $\alpha = -0.1$ ($p = 0.004$, Bonferroni-corrected t-test), it is possible to reduce mean class selectivity by a factor of 5 with only a 0.5% decrease in test accuracy, and by a factor of 10—to 0.03—with only a $\sim 1\%$ drop in test accuracy. These differences may be due in part to VGG16’s naturally higher levels of class selectivity. (see Appendix A.4 for VGG16 results and Appendix A.7 for comparisons between VGG16 and ResNet20). Together, these results demonstrate that class selectivity in individual units is largely unnecessary for optimal performance in DNNs.

Note that we primarily discuss results pertaining to ResNet20 in the main text. Please see Appendix A.4 for complete information about VGG16.

4.2. Does selectivity shift to a different basis set?

We reduced mean class selectivity across the network by an order of magnitude with no significant effect on test accuracy ($p = 0.6$). However, one trivial solution for reducing class selectivity would be for the network to "hide" it from the regularizer by rotating it off of unit-aligned axes or performing some other linear transformation. If the network learned this solution, the selectivity in individual units would be reduced, but remain accessible through linear combinations of activity across units. In order to test possibility, we used CCA (see Approach 3.4), which is invariant to rotation and other invertible affine transformations, to compare the representations in regularized (i.e. low-selectivity) networks to the representations in unregularized networks.

We first established a meaningful baseline for comparison

by computing the CCA distances between each pair of 20 replicate networks for a given value of α (we refer to this set of distances as $\rho(\alpha_r, \alpha_r)$). If regularizing against class selectivity causes the network to move selectivity off-axis, the CCA distances between regularized and unregularized networks—which we term $\rho(\alpha_r, \alpha_0)$ —should be similar to $\rho(\alpha_r, \alpha_r)$. Alternatively, if class selectivity is suppressed via some non-affine transformation of the representation, $\rho(\alpha_r, \alpha_0)$ should exceed $\rho(\alpha_r, \alpha_r)$.

Our analyses confirm the latter hypothesis: we find that $\rho(\alpha_r, \alpha_0)$ significantly exceeds $\rho(\alpha_r, \alpha_r)$ for all values of α (Figure 3; $p < 5 \times 10^6$, paired t-test). Furthermore, the size of the effect is proportional to the regularization scale; larger regularization scales yield representations that are more dissimilar from the unregularized representations. These results support the conclusion that our regularizer doesn’t simply cause class selectivity to be rotated off of unit-aligned axes, but suppresses it. While one may argue that class selectivity has merely undergone some non-invertible and/or non-linear transformation(s), recovering class selectivity in such a scenario is non-trivial and falls outside conventional definitions of class selectivity.

4.3. Increased class selectivity considered harmful

We have demonstrated that class selectivity can be significantly reduced with little to no impact on test accuracy. However, we only examined the effects of *reducing* selectivity. The complement remains unknown: what are the effects of *increasing* selectivity? We examined this question by regularizing *for* class selectivity, instead of against it. This

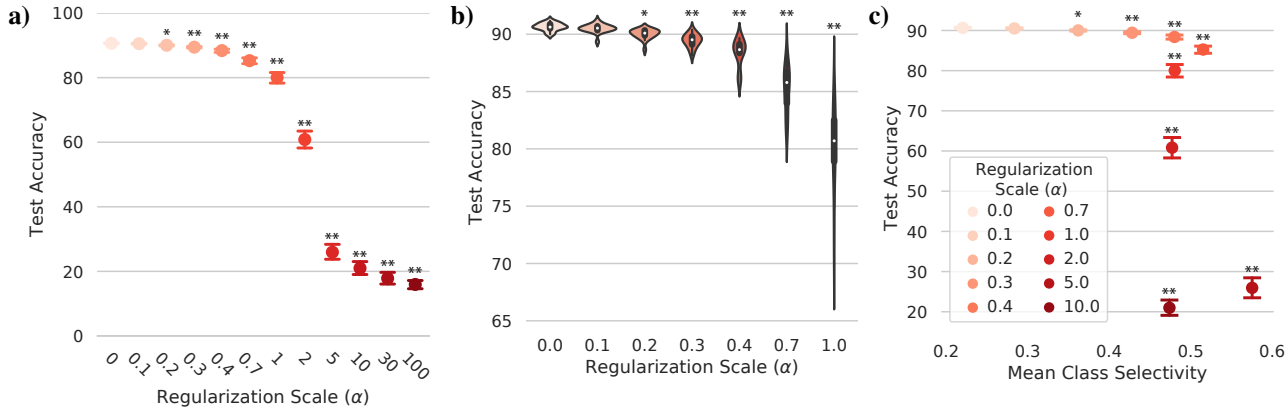


Figure 4: Effects of increasing class selectivity on test accuracy. (a) Test accuracy (y-axis) as a function of regularization scale (α ; x-axis, intensity of red). (b) Identical to (a), but for a subset of α values. The center of each violin plot contains a boxplot, in which the darker central lines denote the central two quartiles. (c) Test accuracy (y-axis) as a function of mean class selectivity (x-axis) for different values of α . Error bars denote 95% confidence intervals. $*p < 2 \times 10^{-4}$, $**p < 5 \times 10^{-7}$ difference from $\alpha = 0$, t-test, Bonferroni-corrected. All results shown are for ResNet20.

is achieved quite easily, as it requires only a change in the sign of α . We first confirmed that changing the sign of the scale term in the loss function causes the intended effect of increasing class selectivity in individual units (see Appendix A.3 and x-axis of Figure 4c). The relationship between α and class selectivity is less consistent for larger values of α , but this will be addressed in the next section (4.4).

Class selectivity does not seem to be strictly necessary for high performance. However, given the ubiquity of class selectivity across biological and artificial neural networks, we suspect it may still be sufficient, in which case we expect increasing it would either improve test accuracy or yield no effect. For the same reason, we would consider it unexpected if increasing selectivity impairs test accuracy.

Surprisingly, however, we observe the latter outcome; increasing class selectivity negatively impacts network performance (Figure 4a). Scaling the regularization has a rapid effect that progresses dramatically: a significant decline in test accuracy emerges at small values of α ($\alpha \geq 0.2$; $p = 0.0001$, Bonferroni-corrected t-test) and falls catastrophically to $\sim 30\%$ by $\alpha = 5.0$.

We observed qualitatively similar results for VGG16 (see Appendix A.4). Although the catastrophic effects of increased class selectivity do not emerge quite as quickly, the decrease in test accuracy is still significant at the smallest tested value of α ($\alpha = 0.1$, $p = 0.02$, Bonferroni-corrected t-test). As mentioned previously, the small differences between ResNet20 and VGG16 could be attributed to VGG16’s naturally higher levels of class selectivity.

These results indicate that increasing class selectivity beyond the levels that are learned without regularization (i.e. $\alpha = 0$) has disastrous effects on network performance.

But what causes this large drop in performance? The inconsistent relationship between α and class selectivity for larger values of α led us to question whether the performance deficits were due to an alternative factor, such as the optimization process, rather than class selectivity per se.

4.4. Single unit necromancy

Lethal ReLUs Interestingly, we observed that networks regularized to increase selectivity contained significantly higher proportions of dead units (see Figure A9a). This is not unexpected, as units with the ReLU activation function are known to suffer from the "dying ReLU problem" (Lu et al., 2019). Removing the dead units makes the relationship between regularization and selectivity more consistent at large regularization scales (see Appendix A.6). The dead units could also explain the decrease in performance as simply a decrease in capacity.

Fruitless resuscitation One solution to the dying ReLU problem is to use a leaky-ReLU activation function (Maas et al., 2013), which has a non-zero slope, b (and thus non-zero gradient) for $x \leq 0$. Accordingly, we re-ran the previous experiment using units with a leaky-ReLU activation in an attempt to control for the potential confound of dead units. If the performance deficits from regularizing for selectivity are simply due to dead units, then using leaky-ReLUs should rescue performance. Alternatively, if dead units are not the cause of the performance deficits, then leaky-ReLUs should not have an effect.

We first confirmed that using leaky-ReLUs solves the dead unit problem. Indeed, the proportion of dead units is reduced to 0 in all networks across all tested values of b . Despite complete recovery of the dead units, however, us-

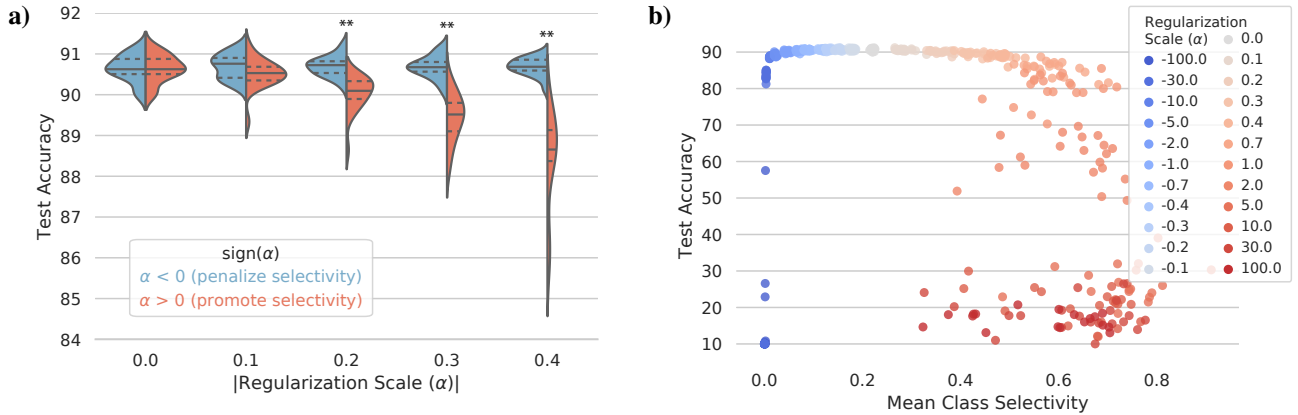


Figure 5: Increasing class selectivity has rapid and deleterious effects on test accuracy compared to reducing class selectivity. (a) Test accuracy (y-axis) as a function of regularization scale magnitude ($|\alpha|$) for negative (blue) vs positive (red) values of α . Solid line in distributions denotes mean, dashed line denotes central two quartiles. $**p < 6 \times 10^{-6}$ difference between $\alpha < 0$ and $\alpha > 0$, Wilcoxon rank-sum test, Bonferroni-corrected. (b) Test accuracy (y-axis) as a function of mean class selectivity (x-axis). All results shown are for ResNet20.

ing leaky-ReLUs does not rescue class selectivity-induced performance deficits (see Figure A10). While the largest negative slope value improved test accuracy for larger values of α , the improvement was minor, and increasing α still had catastrophic effects. These results confirm that dead units cannot explain the rapid and catastrophic effects of increased class selectivity on performance.

4.5. Recapitulation

To fully convey the differences between increasing and decreasing class selectivity, we compare them directly in Figure 5 (also see Appendix A.7 for additional comparisons). Increasing class selectivity significantly impairs test accuracy relative to decreasing class selectivity starting at $|\alpha| = 0.2$ ($p = 5 \times 10^{-6}$, Bonferroni-corrected Wilcoxon rank-sum test). Decreasing selectivity only begins to significantly reduce test accuracy—by $\sim 0.5\%$ —at $\alpha = -2.0$ (Figure 5a), while by $\alpha = 2.0$ test accuracy has already dropped to $\sim 60\%$ (Figure 5b).

5. Discussion

We were able to examine the causal role of class selectivity in neural network performance by adding a term to the loss function that allows us to directly manipulate class selectivity across all the neurons in a DNN. We found that class selectivity is not strictly necessary for networks to function; we could reduce the mean class selectivity of units in a network by factor of ~ 2.5 with no impact on test accuracy, and by a factor of ~ 20 —nearly to a mean of 0—with only a 2% change in test accuracy. We confirmed that our regularizer seems to suppress class selectivity, and not simply cause the network to rotate class selectivity off of unit-aligned axes. We also found that regularizing a network

to increase class selectivity in individual units has disastrous effects on performance. Together, these results demonstrate that class selectivity in individual units is neither necessary nor sufficient for DNNs to function.

5.1. Limitations and future directions

One caveat to our results is that they rely on a single dataset and task: image classification using CIFAR10. It’s possible that our findings are due to data statistics unique to CIFAR10, and wouldn’t generalize to larger and more naturalistic datasets and tasks. Given that class selectivity is ubiquitous across DNNs trained on a variety of tasks and datasets, future work should examine whether the results we report here generalize across tasks and datasets.

Our results make a broader point about the potential pitfalls of focusing on the properties of single units. While we consider it essential to find tractable, intuitive methods of understanding complex systems, it’s also critical that the approaches we take for doing so reflect functionally relevant properties of the system being examined.

We know that class selectivity in individual units naturally emerges over the course of learning. The single unit ablation studies show that class selectivity CAN have an effect on the performance of trained networks. But we demonstrated that it’s not strictly necessary for networks to learn representations that result in class-selective units. This naturally leads to a compelling question: if class selectivity is unnecessary, why does it emerge?

ACKNOWLEDGEMENTS

We would like to thank Tatiana Likhomanenko, Tiffany Cai, Eric Mintun, Janice Lan, Mike Rabbat, and Lyndon Duong

for their productive scrutiny and insightful feedback.

References

- Adrian, E. D. The impulses produced by sensory nerve endings. The Journal of Physiology, 61(1):49–72, March 1926. ISSN 0022-3751. URL <https://www.ncbi.nlm.nih.gov/pmc/articles/PMC1514809/>.
- Amjad, R. A., Liu, K., and Geiger, B. C. Understanding Individual Neuron Importance Using Information Theory. April 2018. URL <https://arxiv.org/abs/1804.06679v3>.
- Barlow, H. B. Single Units and Sensation: A Neuron Doctrine for Perceptual Psychology? Perception, 1(4):371–394, December 1972. ISSN 0301-0066. doi: 10.1068/p010371. URL <https://doi.org/10.1068/p010371>.
- Bau, A., Belinkov, Y., Sajjad, H., Durrani, N., Dalvi, F., and Glass, J. Identifying and Controlling Important Neurons in Neural Machine Translation. In International Conference on Learning Representations, 2019a. URL <https://openreview.net/forum?id=H1z-PsR5KX>.
- Bau, D., Zhou, B., Khosla, A., Oliva, A., and Torralba, A. Network Dissection: Quantifying Interpretability of Deep Visual Representations. In 2017 IEEE Conference on Computer Vision and Pattern Recognition (CVPR), pp. 3319–3327, Honolulu, HI, July 2017. IEEE. ISBN 978-1-5386-0457-1. doi: 10.1109/CVPR.2017.354. URL <http://ieeexplore.ieee.org/document/8099837/>.
- Bau, D., Zhu, J.-Y., Strobel, H., Zhou, B., Tenenbaum, J. B., Freeman, W. T., and Torralba, A. GAN Dissection: Visualizing and Understanding Generative Adversarial Networks. In Proceedings of the International Conference on Learning Representations (ICLR), 2019b.
- Britten, K. H., Shadlen, M. N., Newsome, W. T., and Movshon, J. A. The analysis of visual motion: a comparison of neuronal and psychophysical performance. The Journal of Neuroscience: The Official Journal of the Society for Neuroscience, 12(12):4745–4765, December 1992. ISSN 0270-6474.
- Dalvi, F., Durrani, N., Sajjad, H., Belinkov, Y., Bau, A., and Glass, J. What Is One Grain of Sand in the Desert? Analyzing Individual Neurons in Deep NLP Models. Proceedings of the AAAI Conference on Artificial Intelligence, 33(01):6309–6317, July 2019. ISSN 2374-3468. doi: 10.1609/aaai.v33i01.33016309. URL <https://aaai.org/ojs/index.php/AAAI/article/view/4592>.
- De Valois, R. L., William Yund, E., and Hepler, N. The orientation and direction selectivity of cells in macaque visual cortex. Vision Research, 22(5):531–544, January 1982. ISSN 0042-6989. doi: 10.1016/0042-6989(82)90112-2. URL <http://www.sciencedirect.com/science/article/pii/0042698982901122>.
- Dhamdhere, K., Sundararajan, M., and Yan, Q. How Important is a Neuron. In International Conference on Learning Representations, 2019. URL <https://openreview.net/forum?id=SylKoo0cKm>.
- Donnelly, J. and Roegiest, A. On Interpretability and Feature Representations: An Analysis of the Sentiment Neuron. In Azzopardi, L., Stein, B., Fuhr, N., Mayr, P., Hauff, C., and Hiemstra, D. (eds.), Advances in Information Retrieval, Lecture Notes in Computer Science, pp. 795–802, Cham, 2019. Springer International Publishing. ISBN 978-3-030-15712-8. doi: 10.1007/978-3-030-15712-8_55.
- Erhan, D., Bengio, Y., Courville, A. C., and Vincent, P. Visualizing Higher-Layer Features of a Deep Network. 2009.
- Fong, R. and Vedaldi, A. Net2Vec: Quantifying and Explaining How Concepts are Encoded by Filters in Deep Neural Networks. In 2018 IEEE/CVF Conference on Computer Vision and Pattern Recognition, pp. 8730–8738, Salt Lake City, UT, June 2018. IEEE. ISBN 978-1-5386-6420-9. doi: 10.1109/CVPR.2018.00910. URL <https://ieeexplore.ieee.org/document/8579008/>.
- Fusi, S., Miller, E. K., and Rigotti, M. Why neurons mix: high dimensionality for higher cognition. Current opinion in neurobiology, 37:66–74, 2016. doi: 10.1016/j.conb.2016.01.010. URL <http://eutils.ncbi.nlm.nih.gov/entrez/eutils/elink.fcgi?dbfrom=pubmed&id=26851755&retmode=ref&cmd=prlinks>.
- Gale, E., Blything, R., Martin, N., Bowers, J. S., and Nguyen, A. Selectivity metrics provide misleading estimates of the selectivity of single units in neural networks. In Goel, A. K., Seifert, C. M., and Freksa, C. (eds.), Proceedings of the 41th Annual Meeting of the Cognitive Science Society, CogSci 2019: Creativity + Cognition + Computation, Montreal, Canada, July 24–27, 2019, pp. 1808–1814. cognitivesciencesociety.org, 2019. URL <https://mindmodeling.org/cogsci2019/papers/0319/index.html>.

- Gallego, J. A., Perich, M. G., Naufel, S. N., Ethier, C., Solla, S. A., and Miller, L. E. Cortical population activity within a preserved neural manifold underlies multiple motor behaviors. *Nature Communications*, 9(1):4233, December 2018. ISSN 2041-1723. doi: 10.1038/s41467-018-06560-z. URL <http://www.nature.com/articles/s41467-018-06560-z>.
- Granit, R. Receptors and sensory perception. Receptors and sensory perception. Yale University Press, New Haven, CT, US, 1955.
- He, K., Zhang, X., Ren, S., and Sun, J. Deep residual learning for image recognition. In Proceedings of the IEEE conference on computer vision and pattern recognition, pp. 770–778, 2016.
- Heeger, D. J. and Mackey, W. E. Oscillatory recurrent gated neural integrator circuits (organics), a unifying theoretical framework for neural dynamics. Proceedings of the National Academy of Sciences, 116(45):22783–22794, 2019. ISSN 0027-8424. doi: 10.1073/pnas.1911633116. URL <https://www.pnas.org/content/116/45/22783>.
- Hooker, S., Erhan, D., Kindermans, P.-J., and Kim, B. A Benchmark for Interpretability Methods in Deep Neural Networks. In Wallach, H., Larochelle, H., Beygelzimer, A., Alché-Buc, F. d., Fox, E., and Garnett, R. (eds.), Advances in Neural Information Processing Systems 32, pp. 9734–9745. Curran Associates, Inc., 2019. URL <http://papers.nips.cc/paper/9167-a-benchmark-for-interpretability-methods-in-deep-neural-networks.pdf>.
- Hotelling, H. Relations Between Two Sets of Variates. *Biometrika*, 28(3/4):321–377, 1936. ISSN 0006-3444. doi: 10.2307/2333955. URL <https://www.jstor.org/stable/2333955>.
- Hubel, D. H. Exploration of the primary visual cortex, 1955–78. *Nature*, 299(5883):515–524, October 1982. ISSN 1476-4687. doi: 10.1038/299515a0. URL <https://www.nature.com/articles/299515a0>.
- Hubel, D. H. and Wiesel, T. N. Receptive fields of single neurones in the cat’s striate cortex. *The Journal of Physiology*, 148(3):574–591, 1959. ISSN 1469-7793. doi: 10.1113/jphysiol.1959.sp006308. URL <https://physoc.onlinelibrary.wiley.com/doi/abs/10.1113/jphysiol.1959.sp006308>.
- Hubel, D. H. and Wiesel, T. N. Receptive fields, binocular interaction and functional architecture in the cat’s visual cortex. *The Journal of Physiology*, 160(1):106–154, 1962. ISSN 1469-7793. doi: 10.1113/jphysiol.1962.sp006837. URL <https://physoc.onlinelibrary.wiley.com/doi/abs/10.1113/jphysiol.1962.sp006837>.
- Idelbayev, Y. akamaster/pytorch_resnet_cifar10, January 2020. URL https://github.com/akamaster/pytorch_resnet_cifar10. original-date: 2018-01-15T09:50:56Z.
- Insanally, M. N., Carcea, I., Field, R. E., Rodgers, C. C., DePasquale, B., Rajan, K., DeWeese, M. R., Albanna, B. F., and Froemke, R. C. Spike-timing-dependent ensemble encoding by non-classically responsive cortical neurons. *eLife*, 8:e42409, January 2019. ISSN 2050-084X. doi: 10.7554/eLife.42409. URL <https://doi.org/10.7554/eLife.42409>.
- Kandel, E. R., Schwartz, J. H., and Chao, J. Principles of neural science. McGraw-Hill, New York, 2000.
- Karpathy, A., Johnson, J., and Fei-Fei, L. Visualizing and Understanding Recurrent Networks. In International Conference on Learning Representations, pp. 11, 2016.
- Krizhevsky, A. Learning Multiple Layers of Features from Tiny Images. Technical report, 2009.
- Leavitt, M. L., Pieper, F., Sachs, A. J., and Martinez-Trujillo, J. C. Correlated variability modifies working memory fidelity in primate prefrontal neuronal ensembles. Proceedings of the National Academy of Sciences of the United States of America, 114(12):E2494–E2503, 2017. doi: 10.1073/pnas.1619949114. URL <http://www.pnas.org/lookup/doi/10.1073/pnas.1619949114>.
- Li, Y., Yosinski, J., Clune, J., Lipson, H., and Hopcroft, J. Convergent learning: Do different neural networks learn the same representations? In Storcheus, D., Ros-tamizadeh, A., and Kumar, S. (eds.), Proceedings of the 1st International Workshop on Feature Extraction: Modern Questions and Challenges at NIPS 2015, volume 44 of Proceedings of Machine Learning Research, pp. 196–212, Montreal, Canada, 11 Dec 2015. PMLR. URL <http://proceedings.mlr.press/v44/li15convergent.html>.
- Lillian, P. E., Meyes, R., and Meisen, T. Ablation of a Robot’s Brain: Neural Networks Under a Knife. December 2018. URL <https://arxiv.org/abs/1812.05687v2>.
- Lu, L., Shin, Y., Su, Y., and Karniadakis, G. E. Dying ReLU and Initialization: Theory and Numerical Examples. arXiv:1903.06733 [cs, math, stat], November 2019. URL <http://arxiv.org/abs/1903.06733>. arXiv: 1903.06733.

- Maas, A. L., Hannun, A. Y., and Ng, A. Y. Rectifier nonlinearities improve neural network acoustic models. In *ICML Workshop on Deep Learning for Audio, Speech and Language Processing*, 2013.
- Meyes, R., Lu, M., de Puiseau, C. W., and Meisen, T. Ablation Studies in Artificial Neural Networks. [arXiv:1901.08644 \[cs, q-bio\]](https://arxiv.org/abs/1901.08644), February 2019. URL <http://arxiv.org/abs/1901.08644>. arXiv: 1901.08644.
- Moody, S. L., Wise, S. P., Pellegrino, G. d., and Zipser, D. A Model That Accounts for Activity in Primate Frontal Cortex during a Delayed Matching-to-Sample Task. *Journal of Neuroscience*, 18(1):399–410, January 1998. ISSN 0270-6474, 1529-2401. doi: 10.1523/JNEUROSCI.18-01-00399.1998. URL <https://www.jneurosci.org/content/18/1/399>.
- Morcos, A., Raghu, M., and Bengio, S. Insights on representational similarity in neural networks with canonical correlation. In Bengio, S., Wallach, H., Larochelle, H., Grauman, K., Cesa-Bianchi, N., and Garnett, R. (eds.), *Advances in Neural Information Processing Systems 31*, pp. 5727–5736. Curran Associates, Inc., 2018a. URL <http://papers.nips.cc/paper/7815-insights-on-representational-similarity-in-neural-networks-with-canonical-correlation.pdf>.
- Morcos, A. S. and Harvey, C. D. History-dependent variability in population dynamics during evidence accumulation in cortex. *Nature Neuroscience*, 19(12): 1672–1681, December 2016. ISSN 1546-1726. doi: 10.1038/nn.4403. URL <https://www.nature.com/articles/nn.4403>.
- Morcos, A. S., Barrett, D. G. T., Rabinowitz, N. C., and Botvinick, M. On the importance of single directions for generalization. In *International Conference on Learning Representations*, 2018b. URL <https://openreview.net/forum?id=rliuQjxCZ>.
- Na, S., Choe, Y. J., Lee, D.-H., and Kim, G. Discovery of Natural Language Concepts in Individual Units of CNNs. In *International Conference on Learning Representations*, 2019. URL <https://openreview.net/forum?id=S1EERs09YQ>.
- Nguyen, A., Dosovitskiy, A., Yosinski, J., Brox, T., and Clune, J. Synthesizing the preferred inputs for neurons in neural networks via deep generator networks. In Lee, D. D., Sugiyama, M., Luxburg, U. V., Guyon, I., and Garnett, R. (eds.), *Advances in Neural Information Processing Systems 29*, pp. 3387–3395. Curran Associates, Inc., 2016. URL <http://papers.nips.cc/paper/6519-synthesizing-the-preferred-inputs-for-neurons-in-neural-networks-via-deep-generator-networks.pdf>.
- Olah, C., Mordvintsev, A., and Schubert, L. Feature Visualization. *Distill*, 2(11):e7, November 2017. ISSN 2476-0757. doi: 10.23915/distill.00007. URL <https://distill.pub/2017/feature-visualization>.
- Olah, C., Satyanarayan, A., Johnson, I., Carter, S., Schubert, L., Ye, K., and Mordvintsev, A. The Building Blocks of Interpretability. *Distill*, 3(3):e10, March 2018. ISSN 2476-0757. doi: 10.23915/distill.00010. URL <https://distill.pub/2018/building-blocks>.
- Paszke, A., Gross, S., Massa, F., Lerer, A., Bradbury, J., Chanan, G., Killeen, T., Lin, Z., Gimelshein, N., Antiga, L., Desmaison, A., Kopf, A., Yang, E., DeVito, Z., Raison, M., Tejani, A., Chilamkurthy, S., Steiner, B., Fang, L., Bai, J., and Chintala, S. PyTorch: An Imperative Style, High-Performance Deep Learning Library. In Wallach, H., Larochelle, H., Beygelzimer, A., Alché-Buc, F. d., Fox, E., and Garnett, R. (eds.), *Advances in Neural Information Processing Systems 32*, pp. 8024–8035. Curran Associates, Inc., 2019. URL <http://papers.neurips.cc/paper/9015-pytorch-an-imperative-style-high-performance-deep-learning-library.pdf>.
- Pruszyński, J. A. and Zylberberg, J. The language of the brain: real-world neural population codes. *Current Opinion in Neurobiology*, 58:30–36, October 2019. ISSN 09594388. doi: 10.1016/j.conb.2019.06.005. URL <https://linkinghub.elsevier.com/retrieve/pii/S0959438818302137>.
- Quiñero-Candela, R., Reddy, L., Kreiman, G., Koch, C., and Fried, I. Invariant visual representation by single neurons in the human brain. *Nature*, 435(7045):1102–1107, June 2005. ISSN 1476-4687. doi: 10.1038/nature03687.
- Radford, A., Jozefowicz, R., and Sutskever, I. Learning to Generate Reviews and Discovering Sentiment. [arXiv:1704.01444 \[cs\]](https://arxiv.org/abs/1704.01444), April 2017. URL <http://arxiv.org/abs/1704.01444>. arXiv: 1704.01444.
- Raghu, M., Gilmer, J., Yosinski, J., and Sohl-Dickstein, J. SVCCA: Singular Vector Canonical Correlation Analysis for Deep Learning Dynamics and Interpretability. In Guyon, I., Luxburg, U. V., Bengio, S., Wallach, H., Fergus, R., Vishwanathan, S., and Garnett, R. (eds.), *Advances in Neural Information Processing Systems 30*, pp. 6076–6085. Curran Associates, Inc., 2017.
- Raposo, D., Kaufman, M. T., and Churchland, A. K. A category-free neural population supports evolving

- demands during decision-making. *Nature Neuroscience*, 17(12):1784–1792, 2014. doi: 10.1038/nn.3865. URL <http://eutils.ncbi.nlm.nih.gov/entrez/eutils/elink.fcgi?dbfrom=pubmed&id=25383902&retmode=ref&cmd=prlinks>.
- Saxena, S. and Cunningham, J. P. Towards the neural population doctrine. *Current Opinion in Neurobiology*, 55:103–111, April 2019. ISSN 0959-4388. doi: 10.1016/j.conb.2019.02.002. URL <http://www.sciencedirect.com/science/article/pii/S0959438818300990>.
- Shenoy, K. V., Sahani, M., and Churchland, M. M. Cortical control of arm movements: a dynamical systems perspective. *Annual Review of Neuroscience*, 36:337–359, 2013. doi: 10.1146/annurev-neuro-062111-150509. URL <http://eutils.ncbi.nlm.nih.gov/entrez/eutils/elink.fcgi?dbfrom=pubmed&id=23725001&retmode=ref&cmd=prlinks>.
- Sherrington, C. S. *The integrative action of the nervous system*. The integrative action of the nervous system. Yale University Press, New Haven, CT, US, 1906. doi: 10.1037/13798-000.
- Simonyan, K. and Zisserman, A. Very deep convolutional networks for large-scale image recognition. In Bengio, Y. and LeCun, Y. (eds.), *3rd International Conference on Learning Representations, ICLR 2015, San Diego, CA, USA, May 7-9, 2015, Conference Track Proceedings*, 2015. URL <http://arxiv.org/abs/1409.1556>.
- Simonyan, K., Vedaldi, A., and Zisserman, A. Deep Inside Convolutional Networks: Visualising Image Classification Models and Saliency Maps. *arXiv:1312.6034 [cs]*, April 2014. URL <http://arxiv.org/abs/1312.6034>. arXiv: 1312.6034.
- Smith, S. M., Nichols, T. E., Vidaurre, D., Winkler, A. M., Behrens, T. E. J., Glasser, M. F., Ugurbil, K., Barch, D. M., Van Essen, D. C., and Miller, K. L. A positive-negative mode of population covariation links brain connectivity, demographics and behavior. *Nature Neuroscience*, 18(11):1565–1567, November 2015. ISSN 1546-1726. doi: 10.1038/nn.4125. URL <https://www.nature.com/articles/nn.4125>.
- Sussillo, D., Churchland, M. M., Kaufman, M. T., and Shenoy, K. V. A neural network that finds a naturalistic solution for the production of muscle activity. *Nature Neuroscience*, 18(7):1025–1033, 2015. doi: 10.1038/nn.4042. URL <http://eutils.ncbi.nlm.nih.gov/entrez/eutils/elink.fcgi?dbfrom=pubmed&id=26075643&retmode=ref&cmd=prlinks>.
- Ukita, J. Causal importance of orientation selectivity for generalization in image recognition. September 2018. URL https://openreview.net/forum?id=Bkx_Dj09tQ.
- Virtanen, P., Gommers, R., Oliphant, T. E., Haberland, M., Reddy, T., Cournapeau, D., Burovski, E., Peterson, P., Weckesser, W., Bright, J., van der Walt, S. J., Brett, M., Wilson, J., Millman, K. J., Mayorov, N., Nelson, A. R. J., Jones, E., Kern, R., Larson, E., Carey, C. J., Polat, I., Feng, Y., Moore, E. W., VanderPlas, J., Laxalde, D., Perktold, J., Cimrman, R., Henriksen, I., Quintero, E. A., Harris, C. R., Archibald, A. M., Ribeiro, A. H., Pedregosa, F., van Mulbregt, P., and Contributors, S. . . SciPy 1.0—Fundamental Algorithms for Scientific Computing in Python. *arXiv:1907.10121 [physics]*, July 2019. URL <http://arxiv.org/abs/1907.10121>. arXiv: 1907.10121.
- Waskom, M., Botvinnik, O., O’Kane, D., Hobson, P., Lukauskas, S., Gemperline, D. C., Augspurger, T., Halchenko, Y., Cole, J. B., Warmenhoven, J., Ruiter, J. d., Pye, C., Hoyer, S., Vanderplas, J., Villalba, S., Kunter, G., Quintero, E., Bachant, P., Martin, M., Meyer, K., Miles, A., Ram, Y., Yarkoni, T., Williams, M. L., Evans, C., Fitzgerald, C., Brian, Fonnesbeck, C., Lee, A., and Qalieh, A. *mwaskom/seaborn: v0.8.1* (September 2017), September 2017. URL <https://doi.org/10.5281/zenodo.883859>.
- Wiesel, T. N. Postnatal development of the visual cortex and the influence of environment. *Nature*, 299(5884):583–591, October 1982. ISSN 0028-0836. doi: 10.1038/299583a0.
- Yosinski, J., Clune, J., Nguyen, A., Fuchs, T., and Lipson, H. Understanding Neural Networks Through Deep Visualization. In *ICML Workshop on Visualization for Deep Learning*, 2015. URL <http://arxiv.org/abs/1506.06579>. arXiv: 1506.06579.
- Zeiler, M. D. and Fergus, R. Visualizing and Understanding Convolutional Networks. In Fleet, D., Pajdla, T., Schiele, B., and Tuytelaars, T. (eds.), *Computer Vision – ECCV 2014*, pp. 818–833, Cham, 2014. Springer International Publishing. ISBN 978-3-319-10590-1.
- Zhou, B., Khosla, A., Lapedriza, A., Oliva, A., and Torralba, A. Object Detectors Emerge in Deep Scene CNNs. In *International Conference on Learning Representations*, April 2015. URL <http://arxiv.org/abs/1412.6856>. arXiv: 1412.6856.
- Zhou, B., Sun, Y., Bau, D., and Torralba, A. Revisiting the Importance of Individual Units in CNNs via Ablation. *arXiv:1806.02891 [cs]*, June 2018. URL <http://arxiv.org/abs/1806.02891>. arXiv: 1806.02891.

Zhou, B., Bau, D., Oliva, A., and Torralba, A. Interpreting Deep Visual Representations via Network Dissection. IEEE Transactions on Pattern Analysis and Machine Intelligence, 41(9):2131–2145, September 2019. ISSN 1939-3539. doi: 10.1109/TPAMI.2018.2858759.

Zylberberg, J. The role of untuned neurons in sensory information coding. bioRxiv, pp. 134379, May 2018. doi: 10.1101/134379. URL <https://www.biorxiv.org/content/10.1101/134379v6>.

A. Appendix

A.1. Models, training, dataset, and software

Our experiments were performed on ResNet20 (He et al. (2016)); code modified from Idelbayev (2020) and a VGG16-like network (Simonyan & Zisserman, 2015), both trained on CIFAR10 (Krizhevsky, 2009). The VGG16-like network is identical to the batch norm VGG16 in Simonyan & Zisserman (2015), except the final two fully-connected layers of 4096 units each were replaced with a single 512-unit layer. Models were trained for 200 epochs, using stochastic gradient descent (SGD), with a minibatch size of 256 samples. The ResNet20s were trained with a learning rate of 0.1 and the VGG16 with a learning rate of 0.01, both multiplied (annealed) by 10^{-1} at epochs 100 and 150, with momentum = 0.9 and weight decay = 0.0001. We split the 50k CIFAR10 training samples into a 45k sample training set and a 5k validation set. All experimental results were derived from the test set with the parameters from the epoch that achieved the highest validation set accuracy over 200 training epochs. 20 replicates with different random seeds were run for each hyperparameter set.

Experiments were conducted using PyTorch (Paszke et al., 2019), analyzed using the SciPy ecosystem (Virtanen et al., 2019), and visualized using Seaborn (Waskom et al., 2017).

A.2. CCA

We used Canonical Correlation Analysis (CCA) to examine the effects of class selectivity regularization on representations in neural networks. CCA is a statistical technique that takes two sets of multidimensional variates and finds the linear combinations of these variates that have maximum correlation with each other (Hotelling, 1936). Critically, CCA is invariant to rotation and other invertible affine transformations. CCA has been used in a number of recent studies to analyze and compare representations in (and between) biological and neural networks (Sussillo et al., 2015; Smith et al., 2015; Raghu et al., 2017; Morcos et al., 2018a; Gallego et al., 2018).

For the case of our analyses, let us start with a dataset X , which consists of M data samples $\{x_1, \dots, x_m\}$. Using the notation from Raghu et al. (2017), the scalar output (activation) of a single neuron i on layer l in response to each data sample collectively form the vector

$$z_i^l = (z(x_i^l(x_1), \dots, x_m^l))$$

We then collect the activation vector z_i^l of every neuron in layer l into a matrix $L = \{z_1^l, \dots, z_m^l\}$ of size $N \times M$, N is the number of neurons in layer l , and M is the number of data samples. Given two such activation matrices L_1 , of size $N_a \times M$, and L_2 , of size $N_b \times M$, CCA finds the vectors w (in \mathbb{R}^{N_a}) and s (in \mathbb{R}^{N_b}), such that the inner product

$$\rho = \frac{\langle w^T L_1, s^T L_2 \rangle}{\|w^T L_1\| \cdot \|s^T L_2\|}$$

is maximized.

We use projection-weighted CCA (PWCCA), a variant of CCA introduced in Morcos et al. (2018a) that has been shown to be more robust to noise than traditional CCA and other CCA variants. PWCCA generates a scalar value, ρ , that can be thought of as the distance or dissimilarity between the two sets of multidimensional variates, L_1 and L_2 . For example, if $L_2 = L_1$, then $\rho_{L_1, L_2} = 0$. Now let R be a rotation matrix. Because CCA is invariant to rotation and other invertible affine transformations, if $L_2 = RL_1$ (i.e. if L_2 is a rotation of L_1), then $\rho_{L_1, L_2} = 0$. In contrast, traditional similarity metrics such as Pearson’s Correlation and cosine similarity would obtain different values if $L_2 = L_1$ compared to $L_2 = RL_1$. We use the PWCCA implementation available [here](#), as provided in Morcos et al. (2018a). We hereafter use CCA to refer to PWCCA unless specifically noted.

As an example for the analyses in our experiments, L_1 is the activation matrix for a layer in a network that was not regularized against class selectivity (i.e. $\alpha = 0$), and L_2 is the activation matrix for the same layer in a network that was structured and initialized identically, but subject to regularization against class selectivity (i.e. $\alpha < 0$). If regularizing against class selectivity causes the network’s representations to be rotated (or to undergo to some other invertible affine transformation), then $\rho_{L_1, L_2} = 0$. In practice $\rho_{L_1, L_2} > 0$ due to differences in random seeds and/or other stochastic factors in the training process, so we can determine a threshold value ϵ and say $\rho_{L_1, L_2} \leq \epsilon$. If regularizing against class selectivity instead causes a non-affine transformation to the network’s representations, then $\rho_{L_1, L_2} > \epsilon$.

In our experiments we empirically establish a distribution of ϵ values by computing the PWCCA distances between $\rho_{L_{2a}L_{2b}}$, where L_{2a} and L_{2b} are two networks from the set of 20 replicates for a given hyperparameter combination that differ only in their initial random seed values (and thus have the same α). This gives $\binom{20}{2} = 190$ values of ϵ . We then compute the PWCCA distance between each $\{L_1, L_2\}$ replicate pair, yielding a distribution of $20 \times 20 = 400$ values of ρ_{L_1, L_2} , which we compare to the distribution of ϵ .

A.3. Regularizing to increase class selectivity in ResNet20

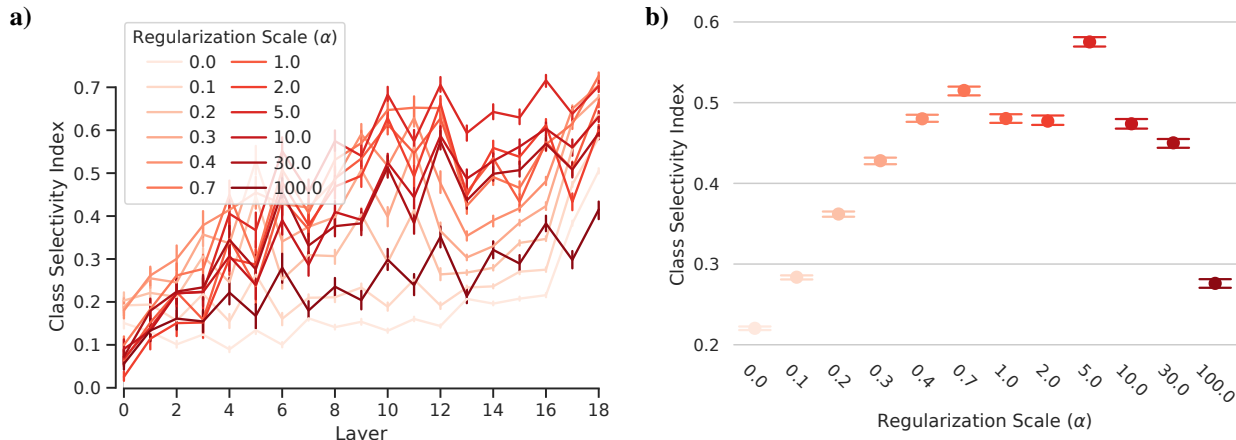


Figure A1: Regularizing to increase class selectivity in ResNet20. (a) Mean class selectivity index (y-axis) as a function of layer (x-axis) for different regularization scales (α ; denoted by intensity of red) for ResNet20. (b) Similar to (a), but mean is computed across all units in a network instead of per layer. Note that the inconsistent effect of larger α values is addressed in Appendix A.6. Error bars denote bootstrapped 95% confidence intervals.

A.4. Results for VGG16

Modulating class selectivity in VGG16 yielded results qualitatively similar to those we observed in ResNet20. The regularizer reliably decreases class selectivity for negative values of α (Figure A2), and class selectivity can be drastically reduced with little impact on test accuracy (Figure A3). Although test accuracy decreases significantly at $\alpha = -0.1$ ($p = 0.004$, Bonferroni-corrected t-test), the effect is small: it is possible to reduce mean class selectivity by a factor of 5 with only a 0.5% decrease in test accuracy, and by a factor of 10—to 0.03—with only a $\sim 1\%$ drop in test accuracy.

Regularizing to increase class selectivity also has similar effects in VGG16 and ResNet20. Increasing α causes class selectivity to increase, and the effect becomes less consistent at large values of α (Figure A1). Although the class selectivity-induced collapse in test accuracy does not emerge quite as rapidly in VGG16 as it does in ResNet20, the decrease in test accuracy is still significant at the smallest tested value of α ($\alpha = 0.1$, $p = 0.02$, Bonferroni-corrected t-test), and the effects on test accuracy of regularizing to promote vs. discourage class selectivity become significantly different at $\alpha = 0.3$ ($p = 10^{-4}$, Wilcoxon rank-sum test; Figure A6). Our observations that class selectivity is neither necessary nor sufficient for performance in both VGG16 and ResNet20 indicates that this is likely a general property of CNNs.

It is worth noting that VGG16 exhibits greater class selectivity than ResNet20. In the absence of regularization (i.e. $\alpha = 0$), mean class selectivity in ResNet20 is 0.22, while in VGG16 it is 0.35, a 1.6x increase. This could explain why positive values of α seem to have a stronger effect on class selectivity in VGG16 relative to ResNet20 (compare Figure A1 and Figure A4; also see Figure A12b).

Selectivity considered harmful: evaluating the causal impact of class selectivity in DNNs

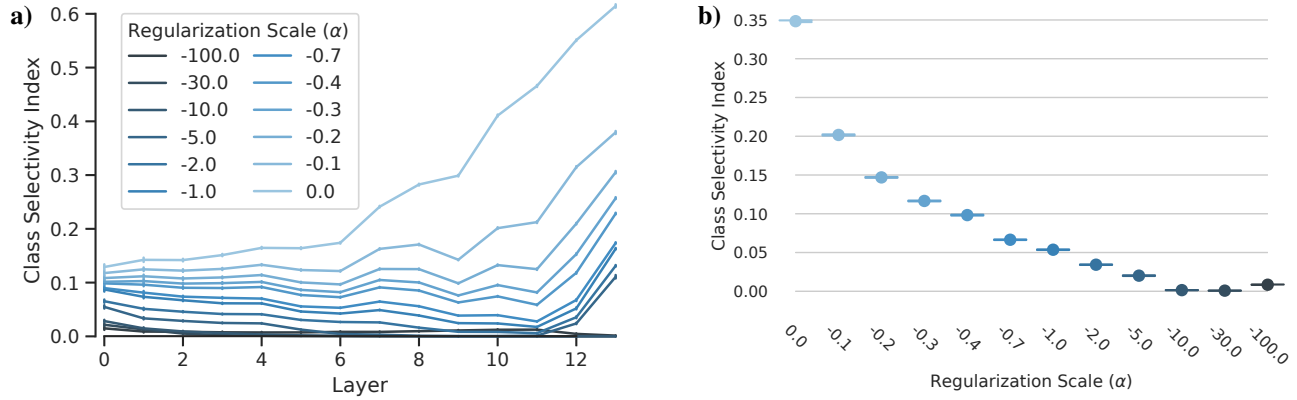


Figure A2: Regularizing to decrease class selectivity in VGG16. (a) Mean class selectivity index (y-axis) as a function of layer (x-axis) for different regularization scales (α ; denoted by intensity of blue) for VGG16. (b) Similar to (a), but mean is computed across all units in a network instead of per layer. Error bars denote bootstrapped 95% confidence intervals.

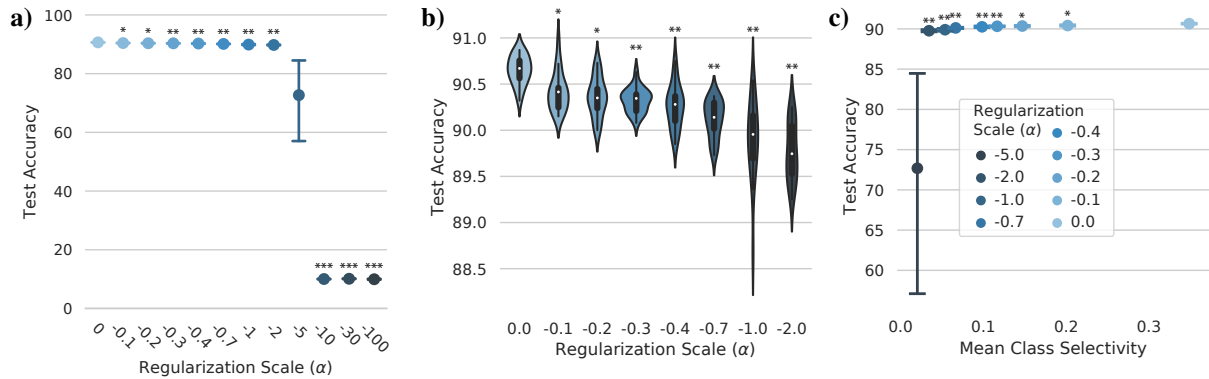


Figure A3: Effects of reducing class selectivity on test accuracy in VGG16. (a) Test accuracy (y-axis) as a function of regularization scale (α , x-axis and intensity of blue). (b) Identical to (a), but for a subset of α values. The center of each violin plot contains a boxplot, in which the darker central lines denote the central two quartiles. (c) Test accuracy (y-axis) as a function of mean class selectivity (x-axis) for different values of α . Error bars denote 95% confidence intervals. $*p < 0.005$, $**p < 5 \times 10^{-6}$, $***p < 5 \times 10^{-60}$ difference from $\alpha = 0$, t-test, Bonferroni-corrected. All results shown are for VGG16.

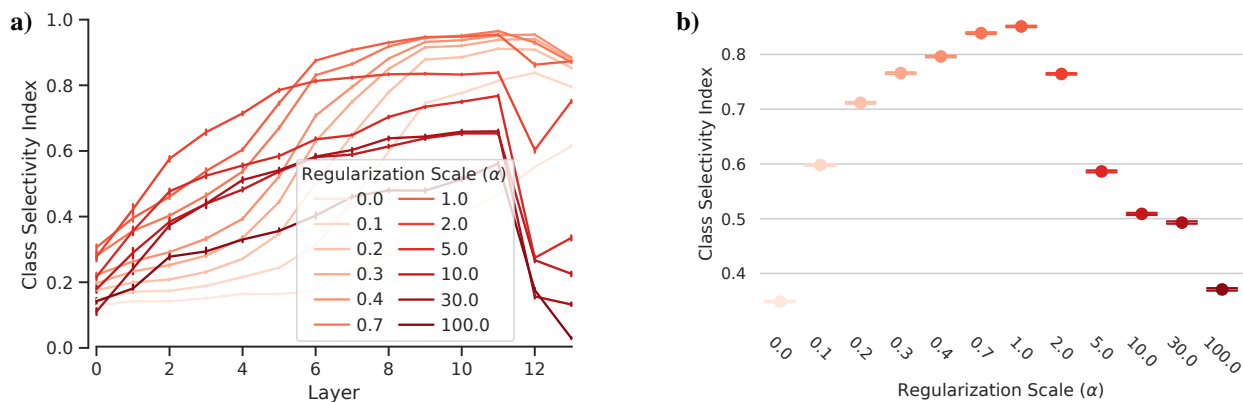


Figure A4: Regularizing to increase class selectivity in VGG16. (a) Mean class selectivity index (y-axis) as a function of layer (x-axis) for different regularization scales (α ; denoted by intensity of red) for VGG16. (b) Similar to (a), but mean is computed across all units in a network instead of per layer. Error bars denote bootstrapped 95% confidence intervals.

Selectivity considered harmful: evaluating the causal impact of class selectivity in DNNs

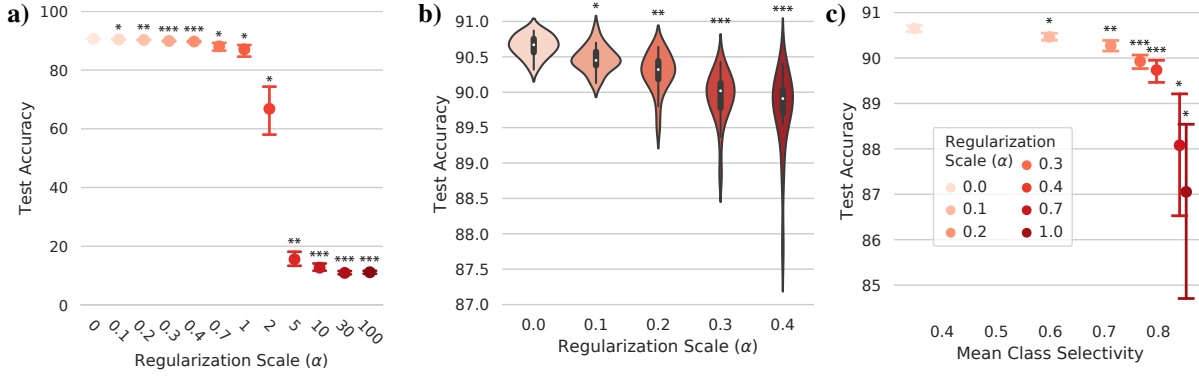


Figure A5: Effects of increasing class selectivity on test accuracy in VGG16. (a) Test accuracy (y-axis) as a function of regularization scale (α , x-axis and intensity of red). (b) Identical to (a), but for a subset of α values. The center of each violin plot contains a boxplot, in which the darker central lines denote the central two quartiles. (c) Test accuracy (y-axis) as a function of mean class selectivity (x-axis) for different values of α . Error bars denote 95% confidence intervals. * $p < 0.05$, ** $p < 5 \times 10^{-4}$, *** $p < 9 \times 10^{-6}$ difference from $\alpha = 0$, t-test, Bonferroni-corrected. All results shown are for VGG16.

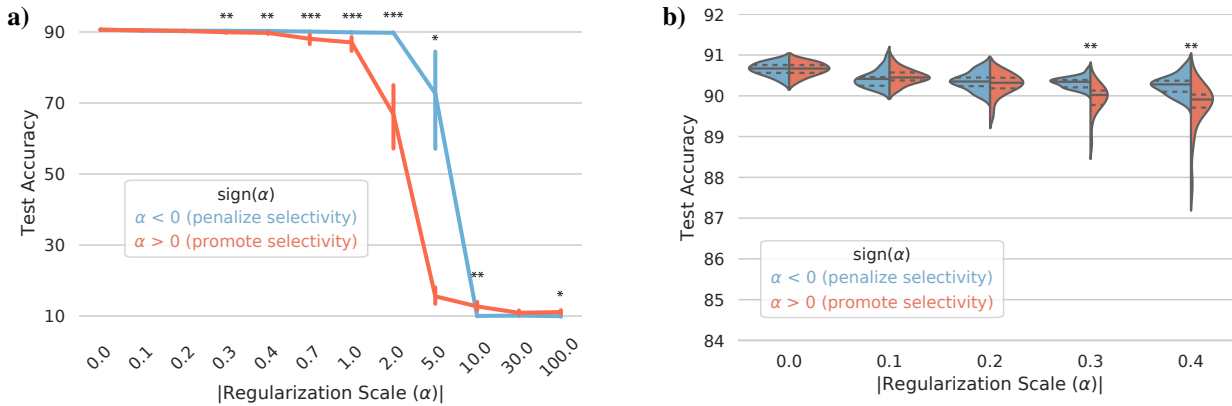


Figure A6: Regularizing to promote vs. penalize class selectivity in VGG16. (a) Test accuracy (y-axis) as a function of regularization scale magnitude ($|\alpha|$; x-axis) when promoting ($\alpha > 0$, red) or penalizing ($\alpha < 0$, blue) class selectivity in VGG16. Error bars denote bootstrapped 95% confidence intervals. (b) Identical to (a), but for a subset of $|\alpha|$ values. * $p < 0.05$, ** $p < 10^{-3}$, *** $p < 10^{-6}$ difference between $\alpha < 0$ and $\alpha > 0$, Wilcoxon rank-sum test, Bonferroni-corrected.

A.5. Different selectivity metrics

In order to confirm that the effect of the regularizer is not unique to our chosen class selectivity metric, we also examined the effect of our regularizer on the "precision" metric for class selectivity (Zhou et al., 2015; 2018; Gale et al., 2019). The precision metric is calculated by finding the N images that most strongly activate a given unit, then finding the image class C_i that constitutes the largest proportion of the N images. Precision is defined as this proportion. For example, if $N = 200$, and the "cats" class, with 74 samples, constitutes the largest proportion of those 200 activations for a unit, then the precision of the unit is $\frac{74}{200} = 0.34$. Note that for a given number of classes C , precision is bounded by $[\frac{1}{C}, 1]$, thus in our experiments the lower bound on precision is 0.1.

Zhou et al. (2015) used $N = 60$, while Gale et al. (2019) used $N = 100$. We chose $N = 1000$, the which is the number of samples per class in the test set data and thus the largest possible sample size.

The class selectivity regularizer has similar effects on precision as it does on the class selectivity index. Regularizing against class selectivity has a consistent effect on precision (Figure A7, while regularizing to promote class selectivity has a consistent effect for smaller values of α , but becomes less consistent for larger values of α . One explanation for the decrease in precision at large values of α is that activation sparsity is a valid solution for maximizing the class selectivity index but not precision. For example, a unit that responded only to ten samples from the class "cat" and not at all to the remaining samples would have a class selectivity index of 1, but a precision value of 0.11.

While there are additional class selectivity metrics that we could have used to further assess the effect of our regularizer, many of them are based on relating the activity of a neuron to the accuracy of the network’s output(s) (e.g. top class selectivity Gale et al. (2019) and class correlation Li et al. (2015); Zhou et al. (2018)), confounding classification accuracy and class selectivity. Accordingly, these metrics are unfit for use in experiments that examine the relationship between class selectivity and classification accuracy, which is exactly what we do here.

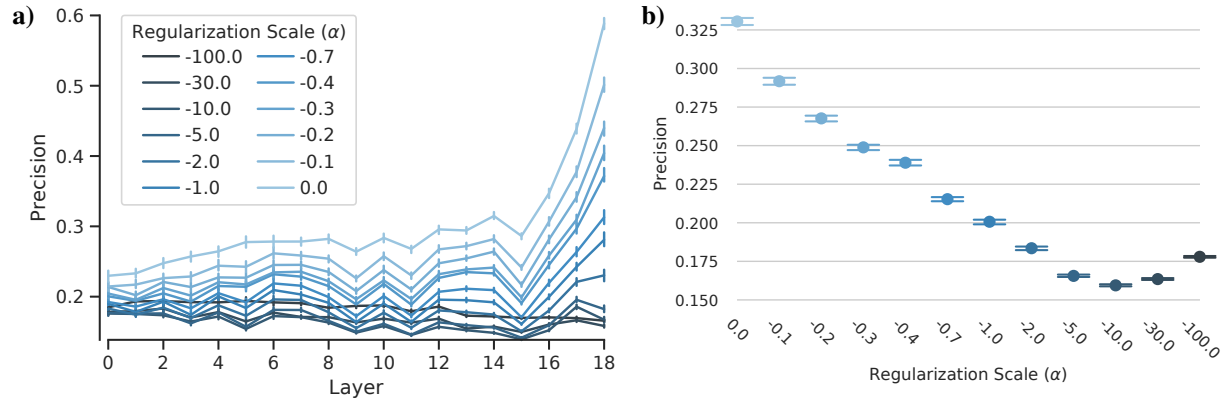


Figure A7: Regularizing against class selectivity has similar effects when measured using a different class selectivity metric. (a) Mean precision (y-axis) as a function of layer (x-axis) for different regularization scales (α ; denoted by intensity of blue) for ResNet20. Precision is an alternative class selectivity metric (see Appendix A.5). (b) Similar to (a), but mean is computed across all units in a network instead of per layer. Error bars denote bootstrapped 95% confidence intervals.

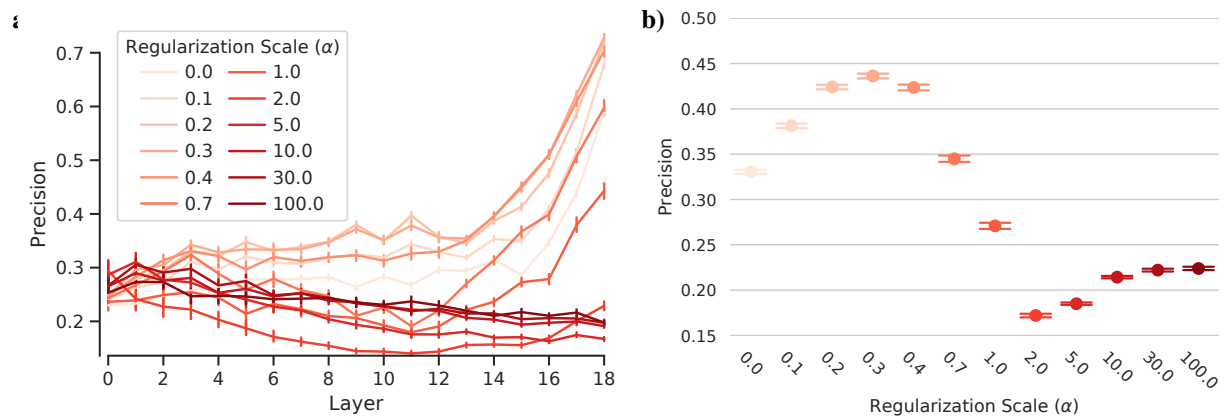


Figure A8: Regularizing to increase class selectivity has similar effects on a different class selectivity metric. (a) Mean precision (y-axis) as a function of layer (x-axis) for different regularization scales (α ; denoted by intensity of red) for ResNet20. (b) Similar to (a), but mean is computed across all units in a network instead of per layer. Error bars denote bootstrapped 95% confidence intervals.

A.6. Impact of dead units

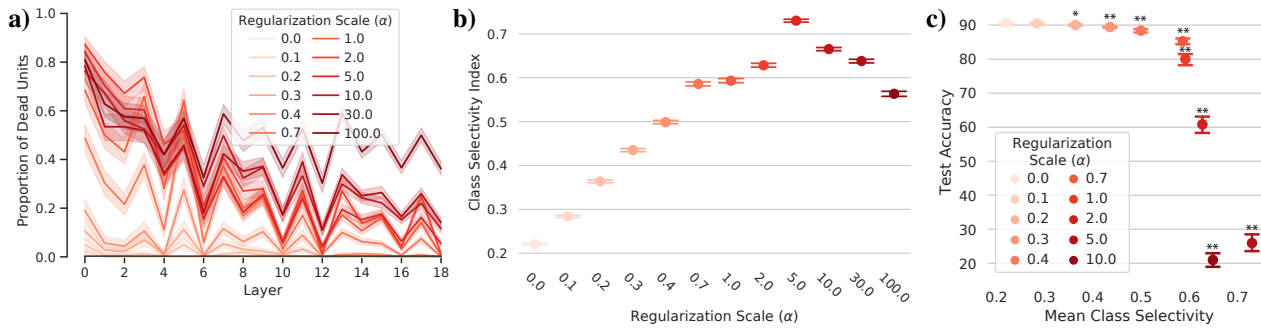


Figure A9: Removing dead units partially stabilizes the effects of large positive regularization scales. (a) Proportion of dead units (y-axis) as a function of layer (x-axis) for different regularization scales (α , intensity of red). (b) Mean class selectivity index (y-axis) as a function of regularization scale (α ; x-axis and intensity of red) after removing dead units. Removing dead units from the class selectivity calculation establishes a more consistent relationship between α and the mean class selectivity index (compare to Figure A1b). (c) Test accuracy (y-axis) as a function of mean class selectivity (x-axis) for different values of α after removing dead units from the class selectivity calculation. Error bars denote 95% confidence intervals. $*p < 2 \times 10^{-4}$, $**p < 5 \times 10^{-7}$ difference from $\alpha = 0$ difference from $\alpha = 0$, t-test, Bonferroni-corrected. All results shown are for ResNet20

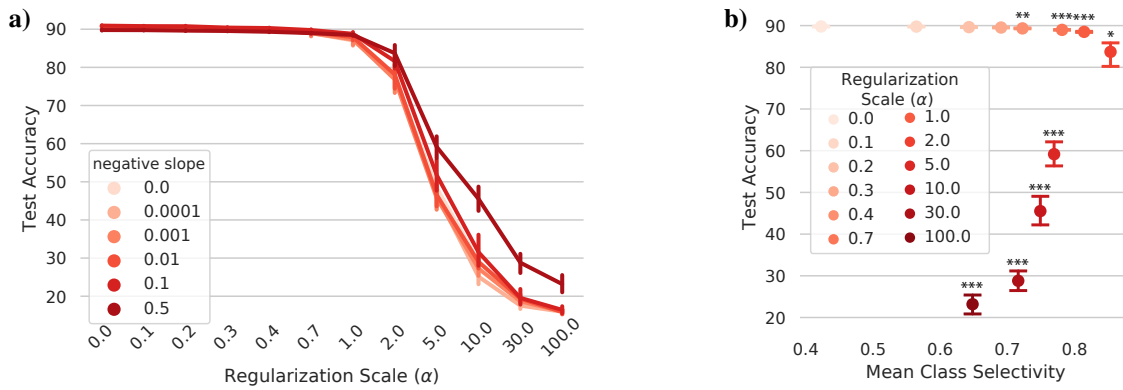


Figure A10: Reviving dead units does not rescue the performance deficits caused by increasing selectivity. (a) Test accuracy (y-axis) as a function of regularization scale (α ; x-axis) for different leaky-ReLU negative slopes (intensity of red). Leaky-ReLUs completely solve the dead unit problem but do not fully rescue test accuracy for networks with $\alpha > 0$. (b) Mean class selectivity index (y-axis) as a function of regularization scale (α ; x-axis and intensity of red) for leaky-ReLU negative slope = 0.5. $*p < 0.001$, $**p < 2 \times 10^{-4}$, $***p < 5 \times 10^{-10}$ difference from $\alpha = 0$, t-test, Bonferroni-corrected. Error bars denote bootstrapped 95% confidence intervals.

A.7. Additional results

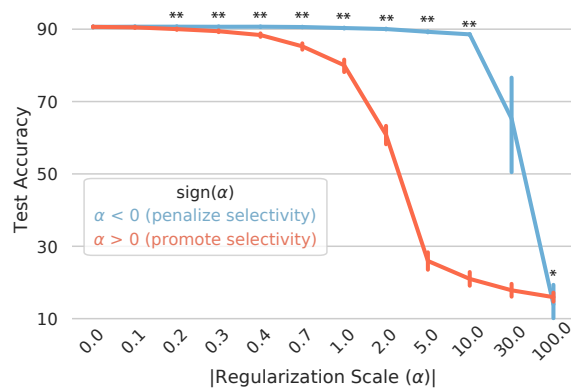


Figure A11: Difference between promoting vs penalizing class selectivity in ResNet20. Test accuracy (y-axis) as a function of regularization scale (α ; x-axis) when promoting ($\alpha > 0$, red) or penalizing ($\alpha < 0$, blue) class selectivity in ResNet20. $*p < 0.05$, $**p < 6 \times 10^{-6}$ difference from $\alpha = 0$, Wilcoxon rank-sum test, Bonferroni-corrected. Error bars denote bootstrapped 95% confidence intervals.

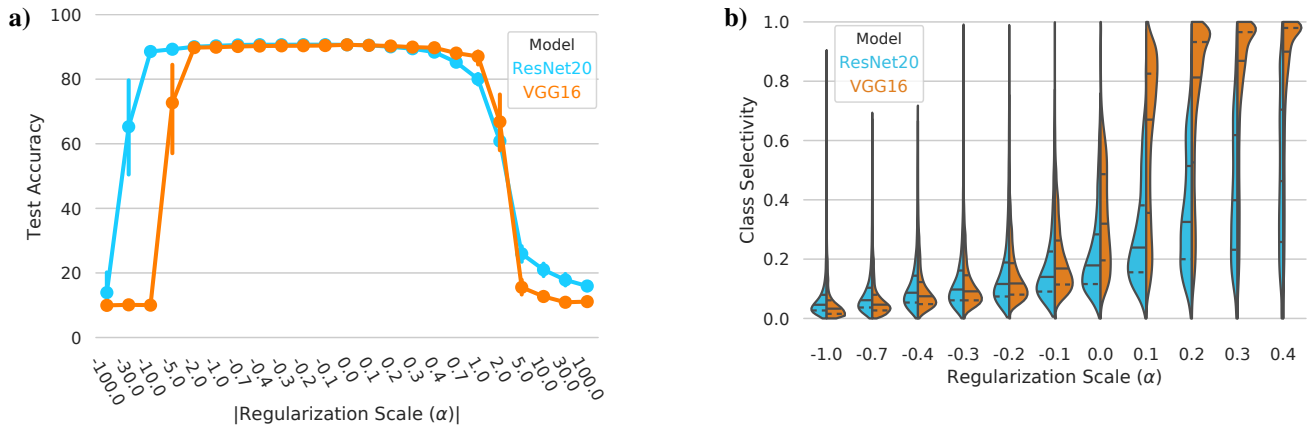


Figure A12: Differences between ResNet20 and VGG16. (a) Test accuracy (y-axis) as a function of regularization scale (α x-axis) for ResNet20 (cyan) and VGG16 (orange). Error bars denote bootstrapped 95% confidence intervals. (b) Class selectivity (y-axis) as a function of regularization scale (α for Resnet20 (cyan) and VGG16 (orange)).